SCIENCE AND TECHNOLOGY ORGANIZATION
CENTRE FOR MARITIME RESEARCH AND EXPERIMENTATION

Reprint Series **CMRE-PR-2014-003**

A relation between multipath group velocity, mode number, and ray cycle distance

Chris H. Harrison

January 2014

Originally published in:

Journal of the Acoustical Society of America, Vol. 132, No. 1, July 2012, pp. 48-55.

About CMRE

The Centre for Maritime Research and Experimentation (CMRE) is a world-class NATO scientific research and experimentation facility located in La Spezia, Italy.

The CMRE was established by the North Atlantic Council on 1 July 2012 as part of the NATO Science & Technology Organization. The CMRE and its predecessors have served NATO for over 50 years as the SACLANT Anti-Submarine Warfare Centre, SACLANT Undersea Research Centre, NATO Undersea Research Centre (NURC) and now as part of the Science & Technology Organization.

CMRE conducts state-of-the-art scientific research and experimentation ranging from concept development to prototype demonstration in an operational environment and has produced leaders in ocean science, modelling and simulation, acoustics and other disciplines, as well as producing critical results and understanding that have been built into the operational concepts of NATO and the nations.

CMRE conducts hands-on scientific and engineering research for the direct benefit of its NATO Customers. It operates two research vessels that enable science and technology solutions to be explored and exploited at sea. The largest of these vessels, the NRV Alliance, is a global class vessel that is acoustically extremely quiet.

CMRE is a leading example of enabling nations to work more effectively and efficiently together by prioritizing national needs, focusing on research and technology challenges, both in and out of the maritime environment, through the collective Power of its world-class scientists, engineers, and specialized laboratories in collaboration with the many partners in and out of the scientific domain.

NOTE: The CMRE Reprint series reprints papers and articles published by CMRE authors in the open literature as an effort to widely disseminate CMRE products. Users are encouraged to cite the original article where possible.

A relation between multipath group velocity, mode number, and ray cycle distance

Chris H. Harrison[a)]
NATO Undersea Research Centre, Viale San Bartolomeo 400, 19126 La Spezia, Italy

(Received 29 August 2011; revised 17 February 2012; accepted 18 May 2012)

Weston's ray invariant or "characteristic time" in a range-dependent environment is exactly equivalent to the Wentzel–Kramers–Brillouin phase integral for ducted normal modes. By considering a ray element it is shown that the ray invariant can also be written in terms of ray cycle distance and cycle time. This leads to a useful formula for group velocity in terms of cycle distance and mode number. Drawing a distinction between the ray and wave interpretation, the Airy phase (i.e., the existence of a group velocity minimum) can be included in this approach. Favorable comparisons are made with group velocities derived from a normal mode model. The relationship is valid for variable sound speed and variable bathymetry, and this is demonstrated numerically. The formula is applicable to active sonar, multipath pulse shape, target signatures, reverberation, tomography, and underwater communications. © *2012 Acoustical Society of America*. [http://dx.doi.org/10.1121/1.4726075]

PACS number(s): 43.30.Bp, 43.30.Cq, 43.30.Es, 43.30.Vh [MS]

I. INTRODUCTION

Multipath ducted propagation consists of many arrivals that follow paths at various elevation angles. These can be thought of in the frequency domain as modal arrivals or in the time domain as a sequence of delayed impulse-like arrivals. Either way, the acoustic energy travels at a group velocity that depends on mode number or, alternatively, on the equivalent ray angle.

For this reason the group velocity influences several aspects of underwater propagation. The waveguide invariant depends on group and phase slownesses (Brown *et al.*, 2005). The resultant striation patterns, seen as source and receiver separate, can be thought of as the result of a stretching and shrinking impulse response (Harrison, 2011), which are therefore dependent on group velocity. Group velocity can be thought of as the speed of energy transport (Biot, 1957; Lighthill, 1965) and, hence, can be expressed in terms of ray cycle time and cycle distance, as well as rate of change of angular frequency with modal wavenumber ($d\omega/dK$). Group velocity is also important in calculating reverberation as it is composed of responses to many scatterers at different ranges. [Strictly reverberation is a function of time although it is often thought of as a function of range (Harrison and Ainslie, 2010).]

In this paper we find a relation between (modal and ray) group velocity and Weston's concept of a "characteristic time" T (Weston, 1959), which he defined in terms of an integral over the water column (depth H) containing ray angle θ and sound speed c,

$$T = \int_0^H \frac{\sin\theta}{c}\, dz. \tag{1}$$

It is understood that depth integration is limited to the region between ray turning points (i.e., real θ). This characteristic time is also a ray invariant that is proportional to the mode number through the Wentzel–Kramers–Brillouin (WKB) phase integral. In other words in a range-dependent environment T is a constant, independent of range. The characteristic time is also the basis of Weston's flux treatment of propagation (Weston, 1980), and one can derive a related propagation formula for range-dependent environments from the point of view of modes, eigenrays, or energy flux (Harrison and Ainslie, 2010). The relationships between these equations, their derivations, and their regimes of validity are interesting in their own right.

In fact, we will see that the integral in Eq. (1) can be equated to a function of ray cycle distance, cycle time, and turning point velocity. The result, which is also range invariant, can be rewritten as an identity relating group velocity, phase velocity, and cycle distance. So we find an analytical expression for group velocity in terms of mode number, modal eigenvalue, frequency, and cycle distance. (As is well known, the ray cycle distance can already be calculated directly from the separation of the eigenvalues.) In a normal mode program that uses group velocities to calculate reverberation truly as a function of time rather than range [for instance, the model NOGRP (Ellis, 1995; Chapman and Ellis, 1983)], one could use the relationship to avoid having to repeat calculations at closely spaced frequencies to estimate $d\omega/dK$.

Generally, the approach to calculating group velocity using this analytical expression has potential to speed up numerical calculations. It is applicable to any underwater acoustics problem where travel times are of interest. This includes active sonar, multipath pulse shape, target signatures, reverberation, tomography, and underwater communications.

II. SOME RANGE-INVARIANT PROPERTIES

A. Ray point of view

Consider the phase change along an infinitesimal ray element at angle θ in a refracting medium with sound speed $c(r, z)$, being a function of range r and depth z. At angular

[a)]Author to whom correspondence should be addressed. Current address: Visiting Professor at Institute of Sound and Vibration Research, University of Southampton, Highfield, Southampton SO17 1BJ, UK. Electronic mail: harrison@nurc.nato.int

frequency ω the total phase can be written in terms of travel time t and also in terms of the wavenumber $k(r, z) = \omega/c$ and its horizontal and vertical components, so

$$\omega\, dt = k\cos\theta\, dr + k\sin\theta\, dz \tag{2}$$

or, dividing through by ω, consider travel time

$$dt = \frac{\cos\theta}{c}\, dr + \frac{\sin\theta}{c}\, dz. \tag{3}$$

We can now integrate from the sea surface to the seabed (at depth H) to find the ray properties for a ray cycle

$$\int_0^{t_c} dt = \int_0^{r_c} \frac{\cos\theta}{c}\, dr + 2\int_0^{H} \frac{\sin\theta}{c}\, dz, \tag{4}$$

where r_c is cycle distance and t_c is cycle time. If we invoke (at least a local) Snell's law then the integrand in the first integral on the right-hand side is independent of depth for the ray and we can write it in terms of the ray turning point velocity or (local) phase velocity $V = c/\cos\theta$, which is related to the horizontal wavenumber K through $V = \omega/K$. So Eq. (4) can be written in terms of the ray cycle distance r_c and the cycle time t_c as

$$t_c = r_c/V + 2\int_0^{H} \frac{\sin\theta}{c}\, dz. \tag{5}$$

We note that already we have an equation that contains the same integral as Weston's characteristic time or ray invariant [Eq. (1)]. As T is invariant with range, so are the other terms that sum to it, i.e.,

$$t_c - r_c/V = 2T = \text{const.} \tag{6}$$

Further, remembering that there is an identity between the group velocity U and the velocity of transport of energy (Biot, 1957), we have

$$U = r_c/t_c, \tag{7}$$

so Eq. (5) can be written in several equivalent ways as

$$t_c\,(1 - U/V) = 2T, \tag{8}$$

$$r_c\left(\frac{1}{U} - \frac{1}{V}\right) = 2T. \tag{9}$$

Equation (1) can also be thought of as the WKB phase integral (Morse and Feshbach, 1953) so that, for the nth mode with horizontal wavenumber K_n, we have

$$\omega T = \omega\int_0^{H} \frac{\sin\theta}{c} dz = \int_0^{H} \sqrt{k^2(z) - K_n^2}\, dz = \pi(n - \varepsilon), \tag{10}$$

where ε is a dimensionless end correction that depends on the upper and lower boundary conditions for the mode, and so

$$\left(\frac{1}{U} - \frac{1}{V}\right) = \frac{n - \varepsilon}{f\, r_c} = \frac{2T}{r_c}. \tag{11}$$

Finally the group velocity is

$$U = \left[\frac{n - \varepsilon}{f\, r_c} + \frac{1}{V}\right]^{-1}. \tag{12}$$

The terms in this equation are all available in a mode model run at a single frequency: mode number n; modal end correction ε (which we will investigate here in more detail later), frequency f; phase velocity $V = \omega/K_n$; ray cycle distance $r_c = 2\pi/|(K_n - K_{n-1})|$ {the latter equation comes directly from differentiating the WKB phase integral [Eq. (10)] with respect to K_n; see Eqs. (B5) and (B6) in Harrison and Ainslie, 2010}. So the usual procedure of calculating the K_n at nearby frequencies to estimate $d\omega/dK_n$ becomes unnecessary.

B. Airy phase: Modal point of view

Equations (10)–(12) are valid as long as ε, which consists of a contribution from the upper and lower ray turning points, can be treated as independent of frequency and angle, which is true for the sea surface ($\varepsilon = 0$) and for refraction turning points ($\varepsilon = 0.25$). They may not be valid when the seabed constitutes one of the duct boundaries. The earlier equations, being ray equations, could be applied simultaneously at one angle over a range of frequencies. In contrast, fixing the mode number implicitly alters the angle and the modal end correction ε with frequency. As a consequence Eq. (12) does not predict an Airy phase (for an individual mode) correctly, but we will rectify this shortly. Throughout this paper we use the term "Airy phase" loosely to label the existence of a group velocity minimum caused by merging of the waterborne paths with the ground wave (see Tolstoy and Clay, 1987). To understand this better we can re-derive Eqs. (9) and (11) by carefully differentiating Eq. (10), i.e.,

$$\pi(n - \varepsilon) = \int_0^{H} \sqrt{k^2(z) - K_n^2}\, dz, \tag{13}$$

with respect to angular frequency ω. Neither n nor H is a function of frequency but k, K, and ε are. So we find

$$\begin{aligned} -\pi\frac{d\varepsilon}{d\omega} &= \int_0^{H} \frac{k\frac{dk}{d\omega} - K\frac{dK}{d\omega}}{\sqrt{k^2 - K_n^2}}\, dz = \int_0^{H} \frac{\frac{k}{c} - \frac{K}{U}}{\sqrt{k^2 - K_n^2}}\, dz \\ &= \int_0^{H} \frac{1}{\omega}\frac{k^2}{\sqrt{k^2 - K_n^2}}\, dz - \int_0^{H} \frac{1}{U}\frac{K}{\sqrt{k^2 - K_n^2}}\, dz. \end{aligned} \tag{14}$$

Writing the latter integral as $r_c/2$, this reduces to

$$r_c\left(\frac{1}{U} - \frac{1}{V}\right) = \frac{2\pi}{\omega}(n - \varepsilon) + 2\pi\frac{d\varepsilon}{d\omega}, \tag{15}$$

which is the same as Eq. (11) except for an extra term involving the derivative of ε.

Following the notation of Tolstoy and Clay (1987), for a half-space where the vertical wavenumber in the water is γ_w, [$\gamma_w^2 = k_w^2 - K^2$; $k_w = k(H)$; amplitude $\propto \exp(i\gamma_w z)$] and the counterpart in the bottom is g_b, [$g_b^2 = K^2 - k_b^2$; k_b is wavenumber in the seabed; amplitude $\propto \exp(-g_b z)$] with densities in the water and bottom of, respectively, ρ_w and ρ_b

($a = \rho_w/\rho_b$) the end correction ε as derived from the boundary conditions is

$$\varepsilon = a \tan\left(\frac{\gamma_w}{a\, g_b}\right) \Big/ \pi. \tag{16}$$

Notice that for a ray it would be legitimate to imagine the angle as remaining constant while changing the frequency. In this case, both γ_w and g_b are proportional to frequency so that the argument of arctan, and consequently ε are *independent of frequency*. Thus, $d\varepsilon/d\omega = 0$ would make Eq. (11) correct for rays. However, for an individual mode, despite this frequency cancellation, the argument of the arctan is still a function of angle, which is itself forced to be a function of frequency for that mode [see, e.g., Eq. (10)].

Even though we have taken the sound speed in the water to be stratified we will adopt this half-space description of the interaction at the bottom boundary. Explicitly, the derivative of ε at the boundary is

$$-\pi \frac{d\varepsilon}{d\omega} = \frac{1}{a\gamma_w g_b \left(g_b^2 + (\gamma_w/a)^2\right)} \times \left[\frac{K}{U}(g_b^2 + \gamma_w^2) - (g_b^2 k_w^2 + \gamma_w^2 k_b^2)/\omega\right]. \tag{17}$$

This can be substituted in Eq. (15) and the group velocity separated out to reveal, after some manipulation

$$U = \frac{\omega\left(r_c \gamma_w g_b (a^2 g_b^2 + \gamma_w^2) + 2aK(g_b^2 + \gamma_w^2)\right)}{\left(2\pi(n-\varepsilon) + r_c K\right)\gamma_w g_b (a^2 g_b^2 + \gamma_w^2) + 2a(g_b^2 k_w^2 + \gamma_w^2 k_b^2)}. \tag{18}$$

More explicitly the cycle distance and the leading term in the denominator can be written in terms of integrals over the water column

$$r_c = 2K \int_0^H 1/\gamma(z)\, dz \tag{19}$$

and

$$2\pi(n-\varepsilon) + r_c K = 2\int_0^H \gamma(z)\, dz + 2K^2 \int_0^H 1/\gamma(z)\, dz = 2\int_0^H k(z)^2/\gamma(z)\, dz. \tag{20}$$

Equation (18) can also be written as

$$UV = {c_w}^2 \frac{A g_b (a^2 g_b^2 + \gamma_w^2) + a(g_b^2 + \gamma_w^2)}{B g_b (a^2 g_b^2 + \gamma_w^2) + a(g_b^2 + \gamma_w^2 c_w^2/c_b^2)}, \tag{21}$$

where

$$A = \gamma_w \int_0^H 1/\gamma(z)\, dz, \tag{22}$$

$$B = \frac{\gamma_w}{{k_w}^2} \int_0^H \frac{k^2(z)}{\gamma(z)}\, dz. \tag{23}$$

Equations (18) and (21) are valid for a locally stratified water column bounded by a simple half-space seabed. Through Eq. (13) with fixed n [as opposed to Eq. (1) with fixed T] it is also valid for mild changes in the environment, equivalent to the adiabatic approximation. If we insert the values for isovelocity, i.e., $A = H$ and $B = H$, we obtain exactly the same formula as Eq. (4.43) in Tolstoy and Clay (1987), namely,

$$UV = {c_w}^2 \frac{H g_b (a^2 g_b^2 + \gamma_w^2) + a(g_b^2 + \gamma_w^2)}{H g_b (a^2 g_b^2 + \gamma_w^2) + a(g_b^2 + \gamma_w^2 c_w^2/c_b^2)}. \tag{24}$$

Equation (18) can be compared with Eq. (12) by the slight rearrangement as

$$U = \frac{(1+\delta)}{\left(\frac{2\pi(n-\varepsilon)}{\omega r_c} + \frac{1}{V}(1+\delta)\right)}, \tag{25}$$

where

$$\delta = \frac{2aK(g_b^2 + \gamma_w^2)}{r_c \gamma_w g_b (a^2 g_b^2 + \gamma_w^2)} = \frac{2a(g_b^2 k_w^2 + \gamma_w^2 k_b^2)}{K\, r_c \gamma_w g_b (a^2 g_b^2 + \gamma_w^2)} = \frac{2aK(k_w^2 - k_b^2)}{r_c \gamma_w g_b (a^2 g_b^2 + \gamma_w^2)}. \tag{26}$$

The order of magnitude of δ can be estimated by taking the isovelocity cycle distance to be $r_c = 2H\cot\theta = 2HK/\gamma_w$, and noting that g_b is roughly related to the critical angle through $g_b = \sqrt{K^2 - {k_b}^2} \approx \sqrt{{k_w}^2 - {k_b}^2} = k_w \sin\theta_c$, we have

$$\delta \approx \frac{a}{H k_w \sin\theta_c}. \tag{27}$$

But the denominator is just the highest mode number N that the duct will support. It is also related to Weston's effective depth h [Eq. (5), Weston, 1960; also Eq. (39), Harrison, 2010],

$$h = \frac{1}{a\, k_w \sin\theta_c}, \tag{28}$$

so

$$\delta \approx \frac{a}{N} \approx \frac{a^2 h}{H}. \tag{29}$$

The earlier group velocity formula derived from rays [Eq. (12)] is valid provided either the density in the seabed is much higher than in water ($a \to 0$) or there is a significant number of modes ($N \gg 0$) or the effective depth is small compared with the actual depth ($h \ll H$).

In summary the group velocities given by Eq. (18) or Eq. (25) depend on the local cycle distance in a refracting water column, the ratio of water-to-seabed density, and the properties γ_w just above the seabed boundary and g_b just below it. Horizontal environmental variations are tolerated as long as they are slow on a scale of one ray cycle. Implicit in the treatment of ducting, right from Eq. (1), has been the assumption that losses at the seabed are fairly low, and so the lower half-space necessarily has higher sound speed than

water. If the seabed is strongly layered, then one can often calculate equivalent half-space parameters. One would require seabed sound speeds that are predominantly higher than water, although thin low speed intermediate layers would be allowable. There would still be a dominant low loss up to a critical angle followed by higher loss with more complicated interference. These losses are calculable for multilayers using well-known techniques (Sect. 1.6.4, Jensen *et al.*, 1994).

III. NUMERICAL EXAMPLES

In the following examples we use either Eq. (12) or Eq. (18) for group velocity with the subsidiary integrals evaluated through Eqs. (19) and (20). Equation (12) is used when the ray's lower turning point is refracted, and Eq. (18) when it is reflected. For a given sound speed profile (SSP) and a dummy set of K_n we can evaluate the integral in Eq. (10) for each frequency. Then for each frequency and mode number n we can also evaluate ε using Eq. (16), so by interpolation we can find the value of K_n, which satisfies the equation. This is then fed into all the components of Eq. (18) or (12). The lines in the figures can be distinguished by the fact that the upper curves are phase velocity and the lower curves exhibiting a minimum are group velocity.

A. Isovelocity

Figure 1 shows the group and phase velocities for the first seven modes in a simple, isovelocity, flat bottomed environment with water depth 100 m, $c_w = 1500$ m/s, $c_b = 1600$ m/s, $\rho_w = 1$, $\rho_b = 2$ using Eq. (18). Figure 1 also shows the simple formula, Eq. (12) [or Eq. (25) with δ set to zero] as dashed lines. These deviate at the lowest frequencies because they lack the group velocity minimum associated with the frequency-dependent ε and therefore the Airy phase.

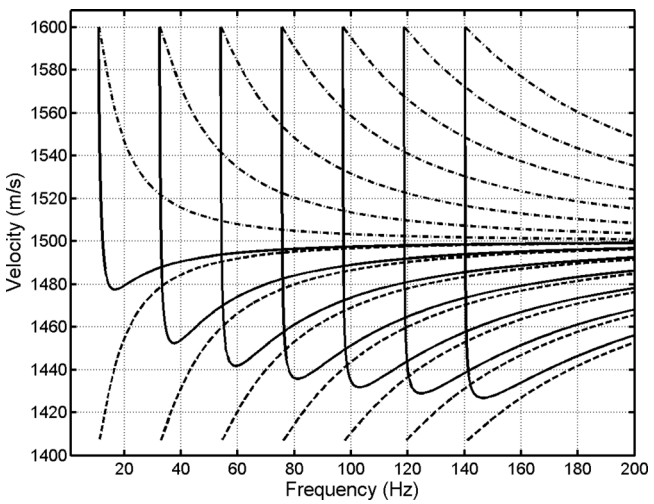

FIG. 1. Group velocities (solid) and phase velocities (dashed-dotted) for the first seven modes [Eq. (18)] for flat bottom, isovelocity, and bottom properties: $c_w = 1500$ m/s, $c_b = 1600$ m/s, $\rho_w = 1$, $\rho_b = 2$. For reference, the simplified group velocities [Eq. (25) with $\delta = 0$] have no Airy phase minimum (dashed).

B. Stratified water column

If the water column is stratified one can separate out four regimes according to ray turning point velocity (i.e., phase velocity) and therefore ray angle. At the upper ray turning point there may be a WKB offset ε_T of either 1/4 for downward refraction or zero for surface reflection (i.e., phase offsets of, respectively, $\pi/4$ or zero). At the lower turning point the WKB offset ε_B may be either 1/4 for upward refraction or ε as in Eq. (16) for bottom reflection. Therefore, for steep angles [phase speeds from c_b down to $\max(c_w)$ including the Airy phase] we expect $\varepsilon_T + \varepsilon_B = \varepsilon$ as in Eq. (16). Then for upward refracted rays trapped in a surface duct, we have $\varepsilon_T + \varepsilon_B = 1/4$, but for downward refracted rays in a bottom duct we have $\varepsilon_T + \varepsilon_B = 1/4 + \varepsilon$. Finally for a sound channel we have $\varepsilon_T + \varepsilon_B = 1/2$. There will be a slight jump in this offset (from the point of view of the earlier equations, but not from the point of view of strict modal propagation) as we go from one regime to another.

C. Downward refraction

The transition from reflected–reflected to downward refracted is illustrated in the following example, superimposing results on a modal solution [using the propagation model ORCA (Westwood *et al.*, 1996)]. There is a uniform gradient between 1500 m/s at the surface and 1480 m/s at the seabed (100 m deep), where bottom properties are the same as in Fig. 1. Figure 2(a) shows the result for the first mode (which is pushing the WKB solution to the limit). The line with an Airy phase minimum and slope discontinuity at ~52 Hz is group velocity calculated using the ε from Eq. (16) alone for all angles. Steep angles are to the left and shallow angles are to the right, and this discontinuity occurs at the above-mentioned transition, in fact when the refracting ray just grazes the sea surface and therefore has phase speed equal to 1500 m/s. The upper phase velocity curve shows that this is indeed true at this frequency. For the reasons stated above, as the ray starts to refract away from the sea surface ε_T jumps from 0 to 1/4, and the dashed line shows the group velocity with this alternative assumption. The thick gray lines are the ORCA mode solutions and we see perfect agreement for low frequencies, through the Airy phase, and then also for high frequencies but with a discrepancy near the transition. Similar observations are true for the phase velocity curve (upper) and its alternative phase curve (dashed). At high frequencies the group velocity begins to decrease with frequency. This strange behavior corresponds exactly with the "sail shaped" deformation of the leading edge of the pulse noted by Harrison and Nielsen (2007). The earliest arrival comes from the vicinity of the transition, i.e., refracted rays that just graze the surface. Any other refracted rays and steeply reflected rays are all slower.

Figure 2(b) shows the equivalent plot for the second mode. Because of the relationship between mode number, angle, and frequency [see Eq. (10)] the transition point (slope discontinuity in group velocity) moves out with frequency even though the ray angle at the transition remains the same. In Eq. (10) the depth integral is a constant, whereas n has changed. Thus, but for minor differences in ε at the two frequencies, the transition frequency is proportional to n.

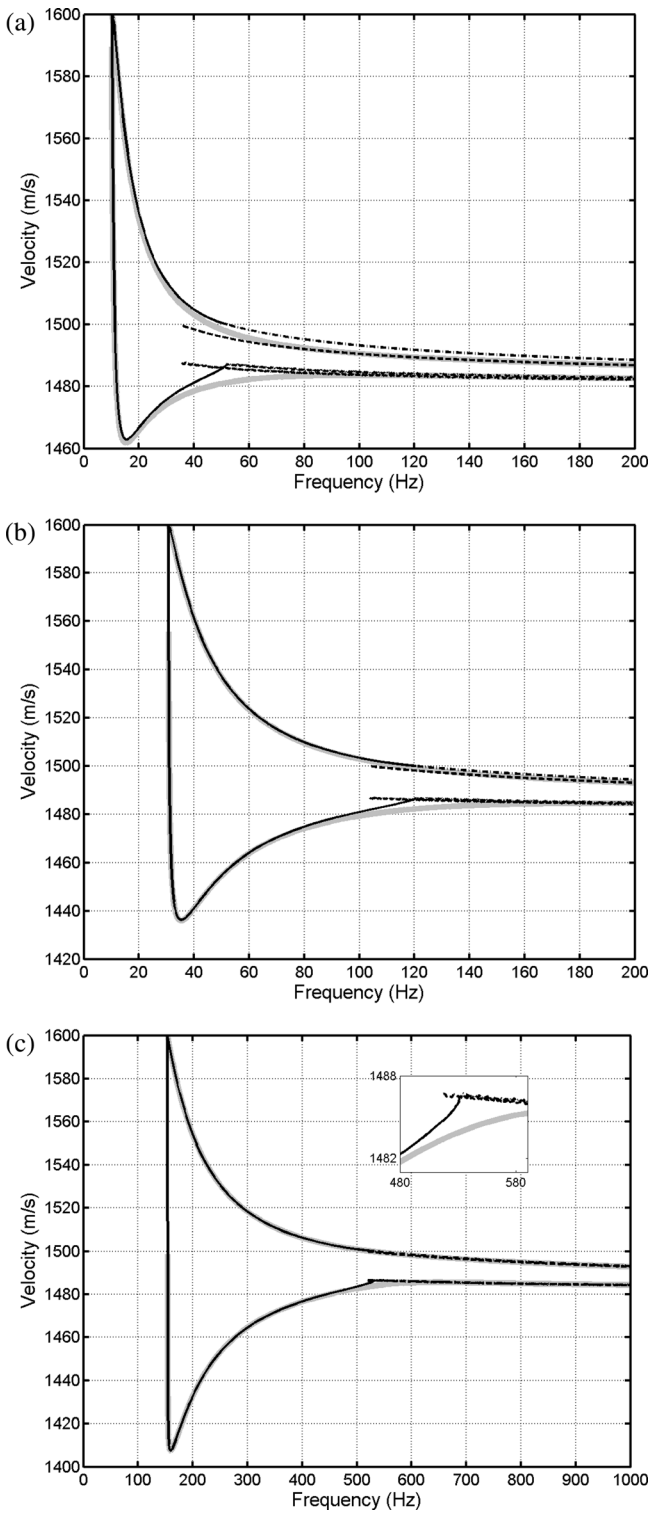

FIG. 2. Group velocity (lower solid) and phase velocity (upper solid) vs frequency [Eq. (18)] for flat bottom with downward refraction superimposed on ORCA normal mode equivalents (thick gray): (a) Mode 1, (b) mode 2, and (c) mode 8. To the right of the discontinuity the rays have an upper refraction turning point, and an additional WKB offset of 1/4 (dashed) brings the formula into alignment with ORCA. For reference, an offset of zero is also shown (dashed-dotted). Bottom parameters are as in Fig. 1. The inset is an enlargement of the group velocity transition.

Figure 2(c) shows mode number 8, again with normal mode calculation superimposed. The discrepancy between these formulas and the ORCA modal solution clearly diminishes as mode number increases.

Because the phase velocity is equal to the ray's turning point velocity c_T we can always calculate a ray angle θ at the depth of the lowest sound speed. Thus, we can use the following relation:

$$V = c_T = c_{\min}/\cos\theta,$$

rearranged as

$$\theta = a\cos(c_{\min}/V),$$

to plot group velocity against angle as in Fig. 3. In this plot for mode number 8 both the Airy phase and the maximum velocity at the transition kink are still visible, and one can also just see the slight disagreement with the modal solution as in the earlier graphs.

D. Upward refraction

Figure 4 shows a similar example for mode 3 and upward refraction (1480 m/s at the surface and 1500 m/s at the seabed). The transition between reflection at both boundaries and upward refraction occurs when the ray grazes the seabed and phase velocity is 1500 m/s. Clearly the group velocity curve would be incorrect if we were to allow ε_B to be defined by Eq. (16) for rays with refraction turning points. Instead we need to switch to the dashed line for $\varepsilon_T + \varepsilon_B = 1/4$. The ORCA modal solution is shown by the thick gray line, and agreement is excellent away from this transition. Note that with upward refraction there is still a maximum in the group velocity for the same reasons as stated previously for downward refraction.

E. Range variation

The point of this paper has been to show not just that there is a formula for group velocity, but that it can be determined in a range-dependent environment through the relationship to the invariants T (characteristic time) or n (mode

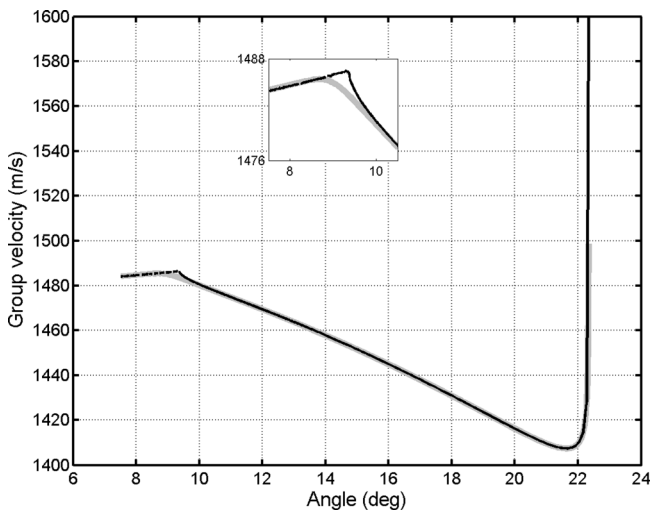

FIG. 3. Group velocity (solid) for mode 8 as in Fig. 2 but plotted against ray angle. ORCA normal mode equivalent (thick gray) and WKB offset of 1/4 (dashed) are also shown. The inset is an enlargement of the group velocity transition.

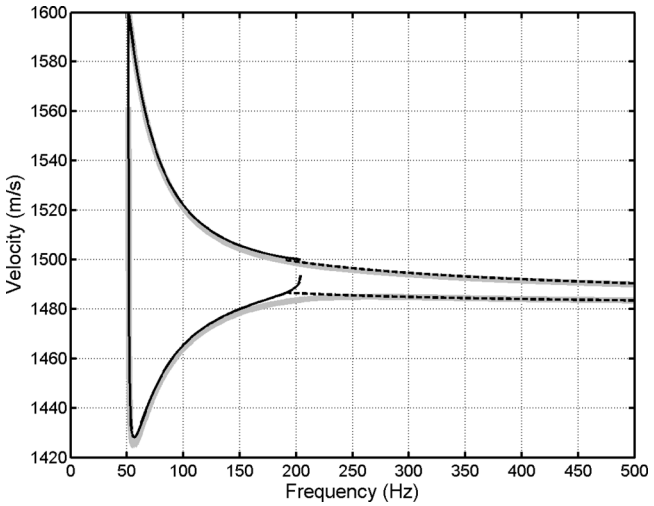

FIG. 4. Group velocity (lower solid) and phase velocity (upper solid) vs frequency for mode 3 [Eq. (18)] for flat bottom with upward refraction superimposed on ORCA normal mode equivalents (thick gray). Dashed lines denote WKB offset of 1/4.

number) [Eq. (11)]. Here we demonstrate the variation of group velocity and phase velocity in an environment where water depth gradually increases from ∼100 to 600 m as in Fig. 5. This is actually a 500 point cubic interpolation between the water depths, 100, 105, 110, 150, 300, 450, 600 m, equally spaced between 0 and 6 km. Bottom properties are the same as assumed earlier. The SSP could also have been range-dependent, but to facilitate comprehension a fixed SSP (Fig. 6) is taken. Sound speeds are piecewise linear between the dots shown.

This particular profile is chosen because, when combined with the varying water depth, it demonstrates all four possible permutations of reflection or refraction at the surface and bottom (i.e., sound channel, upward refraction, downward refraction, surface-bottom reflection). This is possible because the peak surface sound speed of 1506 m/s is reached at the bottom of the duct at depth 331.67 m, so for water depths less than this, i.e., ranges less than 4211 m, downward refraction with bottom reflection is possible,

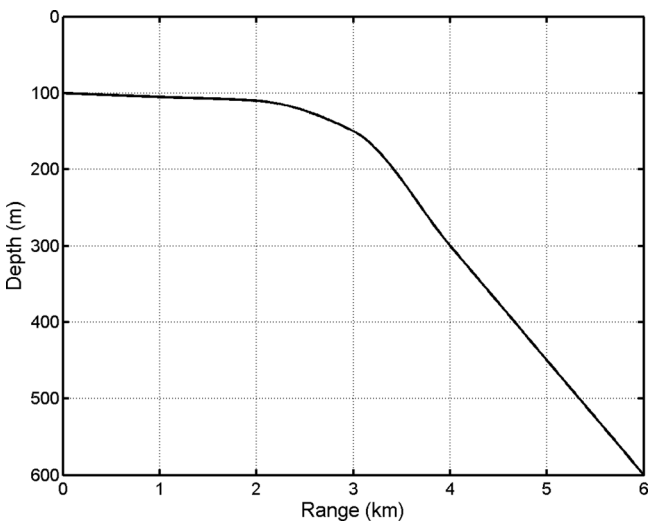

FIG. 5. Bathymetry for the range-dependent case.

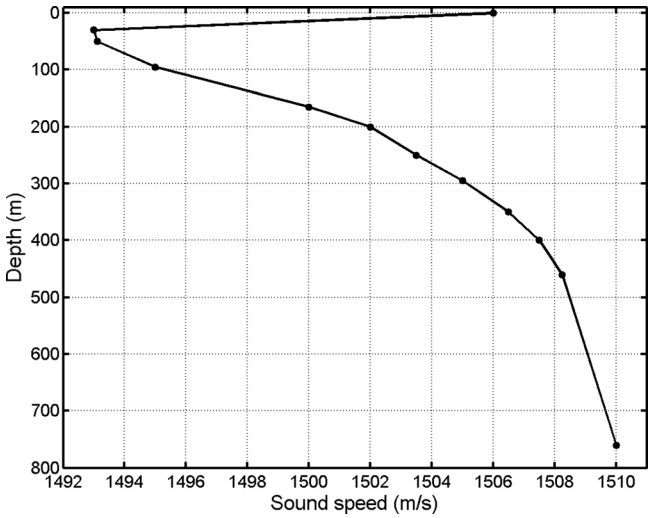

FIG. 6. Fixed sound speed profile for the otherwise range-dependent case.

whereas for greater depths or ranges surface reflection with bottom refraction is possible. Both sound channel and surface-bottom reflection are also possible at all ranges, of course.

Figure 7 shows group and phase velocities vs range at 100 Hz for (a) modes 1–5, (b) modes 6–20. The first five modes are low enough angle that they do not have a group velocity minimum, and as the water deepens they tend to refract away from either boundary, finally entering the sound channel, which can be recognized by the horizontal lines on the right, which can be attributed to the lack of boundary interaction with a fixed sound speed profile.

The curves for modes 6 onward show a distinct group velocity minimum and resemble the earlier plots vs frequency in that mode cutoff for increasing mode number occurs in progressively deeper water. This is because increasing depth has a similar effect on group and phase velocity to increasing frequency [see, e.g., Eq. (11)]. At higher frequencies (not shown) behavior is similar except that there are more modes.

Whether valid or not it is still possible to calculate group and phase velocity assuming all four of the upper and lower turning point conditions separately. We then select the correct one by inspecting the mode amplitude at the sea surface and seabed. This can be deduced from the relative magnitudes of K_n and $k(z)$. Thus, we have

(a) surface reflection $\rightarrow k(0) > K_n$,
(b) surface refraction $\rightarrow k(0) < K_n$,
(c) bottom reflection $\rightarrow k(H) > K_n$, and
(d) bottom refraction $\rightarrow k(H) < K_n$.

At the angle where a refracted ray just grazes the surface or seabed, the first integral in Eq. (10) is a constant. So increasing ε from 0 to 0.25 reduces the frequency slightly. Thus, these "correctly selected" solutions always have a slight overlap in frequency as we have already seen in Fig. 2. This effect translates into an overlap in range, and an enlargement of mode 3 from Fig. 7(a) is shown in Fig. 8 where, passing from left to right, one can clearly see overlapping transitions from reflected–reflected, through

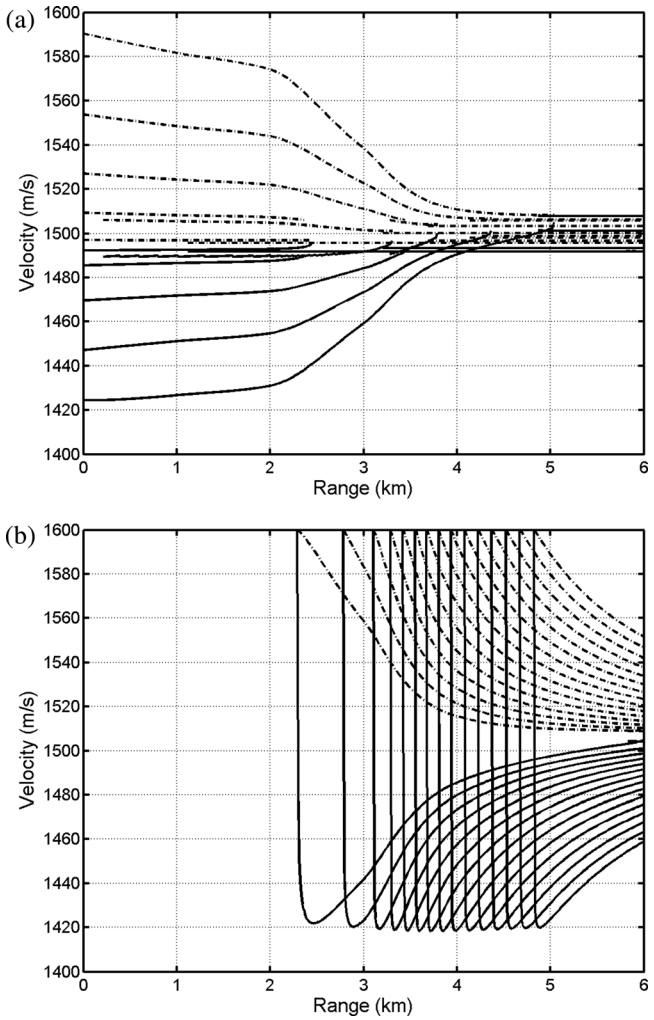

FIG. 7. Variation of group velocity (solid) and phase velocity (dashed-dotted) with range as depth changes according to Fig. 5 with sound speed profile given by Fig. 6 at 100 Hz: (a) Modes 1–5, (b) modes 6–20.

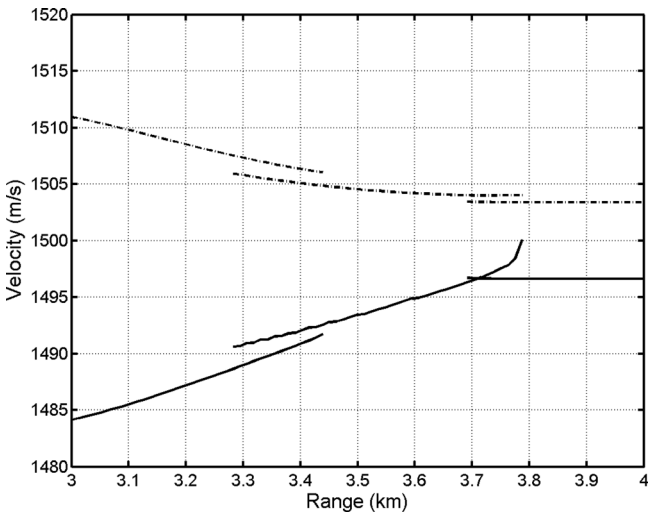

FIG. 8. Enlargement of mode 3 from Fig. 7(a) showing the detailed overlap in range regimes for both group velocity (solid) and phase velocity (dashed-dotted) from reflected–reflected (left), through downward refracted (center), to refracted sound channel (right).

downward refracted, to sound channel. Although comparison with a range-dependent mode model would be interesting, the formulas used here implicitly apply to adiabatic modes, which depend only on the local water depth and sound speed profile. Therefore, in this adiabatic approximation the earlier tests are adequate.

IV. CONCLUSIONS

In a stratified medium phase velocity (i.e., ray turning point velocity) is simply related to the modal eigenvalue and frequency. In most normal mode programs, however, computation of the group velocity for each mode involves computation of eigenvalues at adjacent frequencies. The analytical approach here, based on the WKB "phase integral" and Weston's ray invariant or characteristic time has derived a relationship [Eq. (25), being a generalization of Eqs. (12) and (18)] between group velocity, mode number, ray cycle distance, phase velocity, and frequency. Thus, group velocity can be estimated in a range-dependent environment with less computational effort. Possible applications include active sonar, multipath pulse shape, target signatures, reverberation, tomography, and underwater communications.

The WKB solution in the water column has to be terminated at the depths corresponding to the upper and lower ray turning points, which each may be reflected or refracted. This leads to four possible WKB phase offsets in the phase integral [Eq. (13)], two of which include a group velocity minimum. Although it is clear when each of these is valid, there is a transition from one regime to the other in this scheme. When superimposed on an equivalent normal mode calculation using ORCA (Figs. 2–4) it is seen that agreement is very good away from the transition, particularly for the higher mode numbers. The transition shown in Fig. 2 occurs at a maximum in group velocity, which corresponds to the ray that just grazes the boundary on the high sound speed side of the duct. Both steeper and shallower angle rays are slower than this, as is well known, and this can lead to complicated arrival structures in time.

The relation to Weston's ray invariant is brought out by demonstrating the behavior of group and phase velocity in a range-dependent environment (Fig. 7). Most of the features seen in the earlier frequency plots can also be seen when plotted against range.

ACKNOWLEDGMENT

The author thanks Dr. Peter Nielsen for running the examples with the model ORCA to produce group and phase velocity curves in Figs. 2–4.

Biot, M. A. (**1957**). "General theorems on the equivalence of group velocity and energy transport," Phys. Rev. **105**, 1129–1137.

Brown, M. G., Beron-Vera, F. J., Rypina, I., and Udovydchenkov, I. A. (**2005**). "Rays, modes, wavefield structure, and wavefield stability," J. Acoust. Soc. Am. **117**, 1607–1610.

Chapman, D. M. F., and Ellis, D. D. (**1983**). "The group velocity of normal modes," J. Acoust. Soc. Am. **74**, 973–979.

Ellis, D. D. (**1995**). "A shallow-water normal-mode reverberation model," J. Acoust. Soc. Am. **97**, 2804–2814.

Harrison, C. H. (**2010**). "An approximate form of the Rayleigh reflection loss and its phase: Application to reverberation calculation," J. Acoust. Soc. Am. **128**, 50–57.

Harrison, C. H. (**2011**). "The relation between the waveguide invariant, multipath impulse response, and ray cycles," J. Acoust. Soc. Am. **129**, 2863–2877.

Harrison, C. H., and Ainslie, M. A. (**2010**). "Fixed time versus fixed range reverberation calculation: Analytical solution," J. Acoust. Soc. Am. **128**, 28–38.

Harrison, C. H., and Nielsen, P. L. (**2007**). "Multipath pulse shapes in shallow water: Theory and simulation," J. Acoust. Soc. Am. **121**, 1362–1373.

Jensen, F. B., Kuperman, W. A., Porter, M. B., and Schmidt, H. (**1994**). *Computational Ocean Acoustics* (AIP, New York), pp. 320–323.

Lighthill, M. J. (**1965**). "Group velocity," J. Inst. Math. Appl. **1**, 1–28.

Morse, P. M., and Feshbach, H. (**1953**). *Methods of Theoretical Physics* (McGraw-Hill, New York), p. 1098.

Tolstoy, I., and Clay, C. S. (**1987**). *Ocean Acoustics: Theory and Experiment in Underwater Sound* (AIP, New York), pp. 105–109.

Weston, D. E. (**1959**). "Guided propagation in a slowly varying medium," Proc. Phys. Soc. London **73**, 365–384.

Weston, D. E. (**1960**). "A moiré fringe analog of sound propagation in shallow water," J. Acoust. Soc. Am. **32**, 647–654.

Weston, D. E. (**1980**). "Acoustic flux methods for oceanic guided waves," J. Acoust. Soc. Am. **68**, 287–296.

Westwood, E. K., Tindle, C. T., and Chapman, N. R. (**1996**). "A normal mode model for acousto-elastic ocean environments," J. Acoust. Soc. Am. **100**, 3631–3645.

Document Data Sheet

Security Classification		Project No.
Document Serial No.	**Date of Issue**	**Total Pages**
CMRE-PR-2014-003	January 2014	8 pp.

Author(s)

Harrison, C.H.

Title

A relation between multipath group velocity, mode number, and ray cycle distance

Abstract

Weston's ray invariant or "characteristic time" in a range-dependent environment is exactly equivalent to the Wentzel–Kramers–Brillouin phase integral for ducted normal modes. By considering a ray element it is shown that the ray invariant can also be written in terms of ray cycle distance and cycle time. This leads to a useful formula for group velocity in terms of cycle distance and mode number. Drawing a distinction between the ray and wave interpretation, the Airy phase (i.e., the existence of a group velocity minimum) can be included in this approach. Favorable comparisons are made with group velocities derived from a normal mode model. The relationship is valid for variable sound speed and variable bathymetry, and this is demonstrated numerically. The formula is applicable to active sonar, multipath pulse shape, target signatures, reverberation, tomography, and underwater communications.

Keywords

Issuing Organization

Science and Technology Organization
Centre for Maritime Research and Experimentation

Viale San Bartolomeo 400, 19126 La Spezia, Italy

[From N. America:
STO CMRE
Unit 31318, Box 19, APO AE 09613-1318]

Tel: +39 0187 527 361
Fax:+39 0187 527 700

E-mail: library@cmre.nato.int